HAL
open science

Compressive Sensing for Full Wavefield Image Recovery in Structural Monitoring Applications

Tommaso Di Ianni, Alessandro Perelli, Luca de Marchi, Alessandro Marzani

To cite this version:

Tommaso Di Ianni, Alessandro Perelli, Luca de Marchi, Alessandro Marzani. Compressive Sensing for Full Wavefield Image Recovery in Structural Monitoring Applications. EWSHM - 7th European Workshop on Structural Health Monitoring, IFFSTTAR, Inria, Université de Nantes, Jul 2014, Nantes, France. hal-01022018

HAL Id: hal-01022018

https://inria.hal.science/hal-01022018v1

Submitted on 10 Jul 2014

HAL is a multi-disciplinary open access archive for the deposit and dissemination of scientific research documents, whether they are published or not. The documents may come from teaching and research institutions in France or abroad, or from public or private research centers.

L'archive ouverte pluridisciplinaire **HAL**, est destinée au dépôt et à la diffusion de documents scientifiques de niveau recherche, publiés ou non, émanant des établissements d'enseignement et de recherche français ou étrangers, des laboratoires publics ou privés.

7th European Workshop on Structural Health Monitoring
July 8-11, 2014. La Cité, Nantes, France

COMPRESSIVE SENSING FOR FULL WAVEFIELD IMAGE RECOVERY IN STRUCTURAL MONITORING APPLICATIONS

Tommaso Di Ianni[1], **Alessandro Perelli**[1], **Luca De Marchi**[1], **Alessandro Marzani**[2]

[1] *Dept. of Electrical, Electronic and Information Engineering "Guglielmo Marconi" (DEI), University of Bologna, Bologna, Italy*

[2] *Dept. of Civil, Chemical, Environmental and Materials Engineering (DICAM), University of Bologna, Bologna, Italy*

ABSTRACT

In this paper, a random sampling scheme based on Compressive Sensing (CS) is used in order to reduce the acquisition time of wavefield signals by means of a scanning laser Doppler vibrometer (SLDV) for Structural Health Monitoring (SHM) applications. The sampling process is indeed quite time consuming, because of noise sources and reduced amplitude of acquired signals. By virtue of the sparse characteristic of the wavefield signal representation in terms of sparsity-promoting dictionaries, e.g. Fourier, Curvelet and Wave Atom transforms, the signal can be however recovered through a limited number of measurements. The implemented CS-based procedure has been validated with experimental signals sub-sampled in a pattern of random distributed points, demonstrating the effectiveness of the approach to limit the acquisition time with extremely low information losses.

KEYWORDS : *Compressive Sensing, Lamb waves, Laser vibrometry imaging.*

INTRODUCTION

Guided Waves (GWs) have turned out in recent years to be a suitable tool for Structural Health Monitoring (SHM) applications. In particular, defect detection in plate-like structures through Lamb waves propagation analysis received great attention because of the ability of such waves to propagate long distances with reduced loss in energy [1].

Many Lamb waves applications are based on the inspection of the full wavefield data acquired by means of a scanning laser Doppler vibrometer (SLDV) [2] over the surface of the structure under investigation. In fact, the visualization of the full wavefield propagating into the material provides a wealth of information about the interaction of the wavefronts with structural geometrical features, in particular emphasizing the presence of unexpected discontinuities, e.g. defects. In order to achieve a proper spatial resolution, the field should be sampled in a very fine grid of points. Moreover, because of noise sources and reduced amplitude of acquired signals, multiple temporal measurements are needed at each location to suppress noise content, hence the sampling process requires a huge amount of time.

The Compressive Sensing (CS) [3] theory asserts that if a signal can be expressed in a sparse manner, i.e. its information content can be well-approximated by a linear superimposition of few atomic functions of a proper basis, then such signal can be exhaustively recovered from a limited number of random distributed measurements into a L1 norm minimization procedure. Therefore, the reconstruction performance for each application is mostly influenced by the choice of a proper decomposition basis. Furthermore, the introduction of any constraint in the randomness of the sampling-point distribution provides better reconstruction results, allowing to control the maximum distance between neighbor points, i.e. spatial gap.

In this paper, a CS-based framework is used with the goal of minimize the amount of waveforms collected on the acquisition domain, effectively decreasing the time needed for the sampling stage while preserving the informative content of the wavefield data. At a first stage, two sampling-point

Copyright © Inria (2014)

distribution approaches, both providing random scan-point locations while allowing to control the spatial gap, are tested: Jittered and Farthest Point samplings.

Further, the recovery of the sub-sampled wavefield signal by virtue of several sparsity-promoting dictionaries, namely 2- and 3D Fourier transforms, 2- and 3D Curvelet [4] and Wave Atom [5], is performed in order to estimate the best tradeoff between Signal to Noise Ratio and computational time of the recovery stage. The procedure is tested with a wavefield data obtained experimentally with a scanning laser Doppler vibrometer (SLDV) dataset acquired from a 1.5 mm thick Aluminum plate.

1. Sparsity-promoting Dictionaries

1.1 Fourier transform

The application of multidimensional FTs provides a sparse representation of the wavefield signal [6]. In the frequency-wavenumber domain most components of the acoustic field are indeed concentrated near the surface obtained from the revolution of the dispersion curve.

Many methods were presented before exploiting such sparse characteristic with the goal of improving the visualization of unexpected faults in the structure. In particular, in [7] the FT is used as a valuable tool to separate the incident component, i.e. the exciting wave pulsed by the transducer, by the scattered components introduced by the presence of a defect in the material. The defect is indeed a source of secondary waves exit from its location, which could be completely hidden by the incident wavefront because of their negligible amplitude. Nonetheless, in the frequency-wavenumber domain the incident component can be easily filtered out, allowing a more effective visualization of the residual wave scattered by the defect.

By means of Fast Fourier transforms (FFTs), the decomposition of a discrete N-point signal in the Fourier domain needs $O(N\log_2 N)$ operations.

1.2 Curvelet transform

The Curvelet transform (CT) [8] decomposes a given signal in a linear superimposition of "needle-shaped" functions localized in both spatio-temporal and frequency-wavenumber domains. Identified as curvelets, such functions are equipped with a peculiar selectivity in orientation whereby they are particularly suitable yielding a sparse representation of signals with singularities along curves.

For a 2D signal, the curvelet decomposition is based on a tiling of the frequency-wavenumber domain performed by a couple of smooth, nonnegative and real-valued classes of bandpass functions. Let $\xi = (\xi_1, \xi_2)$ be the Fourier domain variables associated with the spatio-temporal coordinates $x = (x_1, x_2)$. The product of concentric square $\tilde{W}_\nu(\xi)$ and angular $V_{\nu,\ell}(\xi)$ windows defines the Cartesian windows

$$\tilde{U}_{\nu,\ell}(\xi) = \tilde{W}_\nu(\xi) \cdot V_{\nu,\ell}(\xi), \tag{1}$$

where ν and ℓ are two parameters indexing the scale and direction, respectively.

In the Fourier domain, each function in (1) isolates frequencies near the wedge located at the scale $2^{-\nu}$ and oriented in agreement to a set of equispaced directions $\theta_\ell = \ell \cdot 2^{\lfloor \nu/2 \rfloor}$, with $\ell = -2^{\lfloor \nu/2 \rfloor}, \ldots, 2^{\lfloor \nu/2 \rfloor} - 1$. Conversely, in the spatio-temporal domain, a curvelet function is compactly supported in a rectangle centered in $x = (x_1, x_2)$ with major axis orthogonal to the direction θ_ℓ and obeying the *parabolic scaling* relation:

$$length \approx 2^{-\nu/2}, \quad width \approx 2^{-\nu} \quad \Rightarrow \quad width \approx length^2.$$

For a 3D signal the theory is essentially the same, except that in this case the curvelets are supported in a little plate rather than a rectangle. 3D curvelets are suitable representing objects with singularities along smooth curves.

The computational cost of the CT is $O(N\log_2 N)$, and the Curvelab package, which contains the code that computes the Curvelet transform used in this work is available at http://www.curvelet.org.

1.3 Wave Atom transform

Under the assumption that the parabolic scaling is essential to yield good sparsity results, the Wave Atom transform (WA) [5] provides an alternative multiscale strategy for the sparse representation of the full wavefield signal. Following an approach similar to Curvelet transform, the WA performs a dyadic tiling of the frequency-wavenumber domain, decomposing a given signal in a linear superimposition of oscillating functions whose support is approximately a square obeying the parabolic scaling relation:

$$wavelength \approx (width/length)^2.$$

The main feature of the wave atoms is their isotropic aspect ratio $\sim 2^{-\nu/2} \times 2^{-\nu/2}$ in spatio-temporal domain, with oscillations of wavelength $\sim 2^{-\nu}$, as can be noticed in Figure 1.

The computational cost of the WA transform is $O(N \log_2 N)$. Finally, the code performing the WA transform used in this study is available at http://www.waveatom.org.

2. Compressive Sensing

The full wavefield signal can be organized as a 3D data array $u(x_1, x_2, t)$, and the wavefield image at a given time instant t_j is produced taking the 2D slice $u_j = u(x_1, x_2, t_j)$. As stated before, a good visualization of the defect into the plate refers to a proper spatial resolution of the image u_j that hardly involves the time consumption of the sampling process. In the CS approach, the full wavefield signal can be recovered from far fewer measurements than the Shannon/Nyquist theorem suggests.

To better understand how CS works, let us consider a 1D signal $s \in \mathbb{R}^N$, sparse in a proper basis $\Psi \in \mathbb{R}^{N \times N}$, i.e. $s \simeq \Psi \cdot \alpha_k$ with α_k a vector in which all but $k \ll N$ entry are negligible. We are now interested in recovering s from a small set of linear measurements

$$y_i = \langle s, \varphi_i \rangle, \qquad i = 1, \ldots, M \tag{2}$$

with $M \ll N$: the problem is in general ill-posed and admits many solutions. The samples y_i can be then organized as a vector $y \in \mathbb{R}^M$, such that the sampling process can be expressed in a matrix form as

$$y = \Phi \cdot s + z \simeq \Phi\Psi \cdot \alpha_k + z, \tag{3}$$

where $\Phi \in \mathbb{R}^{M \times N}$ is the matrix obtained organizing column-wise the sampling functions φ_i and z is an unknown error term related to both noise and non-idealities.

The CS theory [9] asserts that if Ψ and Φ are sufficiently incoherent, then the signal s can be recovered by solving the basis pursuit denoise (BPDN) problem:

$$\min \|\tilde{\alpha}\|_{\ell_1} \quad \text{subject to} \quad \|\Phi\Psi \cdot \tilde{\alpha} - y\|_{\ell_2} \leq \varepsilon, \tag{4}$$

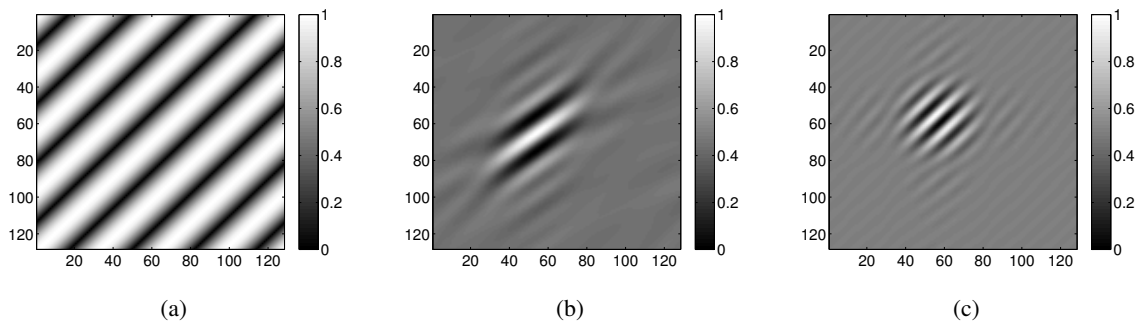

Figure 1: Basis function of the Fourier domain (a); curvelet function (b); and wave atom (c).

where ε bounds the amount of the error term in (3). It can be proven that random waveforms φ_i with independent identically distributed (i.i.d.) entries are rather incoherent with any given dictionary Ψ.

In our approach, a unique pattern of sampling-points random distributed in the acquisition domain is considered for the entire temporal evolution of wavefield propagation. This corresponds to consider $M = 1$ measurements in (2), extending the theory to a 2D case. On the other hand, the temporal waveforms are acquired according to Nyquist rate.

2.1 Sampling-point distribution strategies

In order to deal with the requirement of a spatial gap control, a possible solution is given by Jittered sampling (JS) [10]. The basic idea is to first decimate the starting grid, then randomly perturb the sampling-point positions around the center of each cell of the coarse grid. This way, a uniform probability distribution is considered in each cell at a time rather than on the whole finest grid all at once.

Conversely, Farthest Point sampling (FPS) [11] places in turn the sampling points on the finest grid, progressively selecting the next sample to be the farthest point from all previously selected ones, starting from an initial set of a few random distributed points. FPS leads to a more uniform distribution than JS scheme.

3. Experimental Results

The results of the CS reconstruction of a wavefield signal acquired on a 1.5 mm thick 6061 aluminum plate (638 mm $\times$ 558 mm wide) were compared here in order to assess the proposed approach. The presence of a defect was emulated by a 12 mm diameter cylindrical mass bonded on the surface of the plate. A 20 mm diameter PZT transducer was used to excite the guided field in the structure, while the plate response was recorded through a Polytec PSV400M2 SLDV over a rectangular area of 150 mm $\times$ 155 mm, in a grid of 141 $\times$ 151 equispaced points.

The procedure was implemented in Matlab using the SPGL1 toolbox [12] for the solution of the BPDN problem, with the support of the suite Sparco [13]. As a general rule, the number of iterations of the solving procedure was fixed to allow each time a comparison of the results obtained through different strategies. The outcomes were compared in terms of both computational time and Signal to Noise Ratio, defined as

$$20 \cdot \log_{10} \left(\frac{\|u(x_1, x_2, t)\|}{\|u_r(x_1, x_2, t) - u(x_1, x_2, t)\|} \right),$$

where u_r is the recovered wavefield signal.

In Table 1 the results of the reconstruction in the Fourier domain with 30 iterations of the wavefield signal sub-sampled in 15% locations respect to the original grid, by means of 1- and 2D Jittered distribution and FPS are shown. Even though the Farthest Point strategy produces a more uniform distribution, JS yields a better recovery in terms of SNR.

On the other hand, the Fourier transforms prove to be the best choice as regards the reconstruction dictionary. The recovery in both 2- and 3D Fourier domain reach indeed the best tradeoff between

Table 1: CS reconstruction in the Fourier domain with 30 iterations of the wavefield signal 15% sub-sampled through different sampling-point distribution strategies.

Sampling Scheme	**SNR** [dB]
Jittered 1D	20.64
Jittered 2D	20.67
FPS	19.55

SNR and computational time, as shown in Table 2. In such a case, the solver yet converges with 30 iterations within a few minutes computational time. Conversely, in both Curvelet and Wave Atom 2D domains, the results are mainly similar in terms of SNR, but within several hours computational times. Finally, the recovery in the 3D Curvelet domain produces unsatisfactory results at all.

Table 2: Signal to Noise Ratio and Computational Time of the CS recovery obtained from a full wavefield signal random subsampled in less than 34% locations respect to the original grid distributed with 2D Jittered approach.

Dictionary	**Iterations**	**Computational Time** [min]	**SNR** [dB]
3D FFT	30	2.42	28.38
	90	12.31	28.16
	150	24.37	28.13
2D FFT	30	2.65	26.29
	90	8.99	26.14
	150	14.84	26.11
3D CT	30	29.24	11.41
	90	81.00	18.62
	150	137.85	19.29
2D CT	30	34.95	18.30
	90	101.56	24.22
	150	173.35	24.45
WA	30	94.33	25.93
	90	283.38	29.24
	150	491.90	29.11

In order to supply a visual assessment of the approach, in Figure 2(a) the wavefield image at a given instant of time t_j relative to the full wavefield signal used as a reference is shown along with the recovered ones by the proposed procedure (Fig. 2(b)-(d)). The recovery was performed starting from less than 34% measurements respect to the original grid. It is worth notice the substantial accuracy of all the recovered signals to the acquired one, which de facto prove the effectiveness of the procedure. Furthermore, the current results are by no means achievable directly interpolating the sub-sampled signal.

CONCLUSIONS

In this paper, a CS framework to minimize the number of scan-point locations over the surface of the structure under investigation is presented. Both sampling-point distribution strategies and sparsity-promoting dictionaries were investigated in order to produce the best recovery for a sub-sampled wavefield signal obtained with a scanning laser Doppler vibrometer from a 1.5 mm thick aluminum plate.

The decomposition of the signal in the Fourier domain has turned out to be the more effective solution, leading to a very accurate recovery starting from less than 34% of measurements respect to the original sampling grid within the smallest computational time. The result can be ascribed to the small complexity of the Fourier transform both with the highest incoherence of such dictionary with the examined sampling schemes, and demonstrates the great potential of the CS approach.

Among the future research needs, an adaptive sampling-point distribution strategy could be developed taking advantage of the progressiveness of the FPS scheme. It is possible indeed to introduce case-specific metrics in order to place each new sampling-point in the position that minimize the recovery error, further improving the tradeoff between the amount of sampled data needed to achieve a

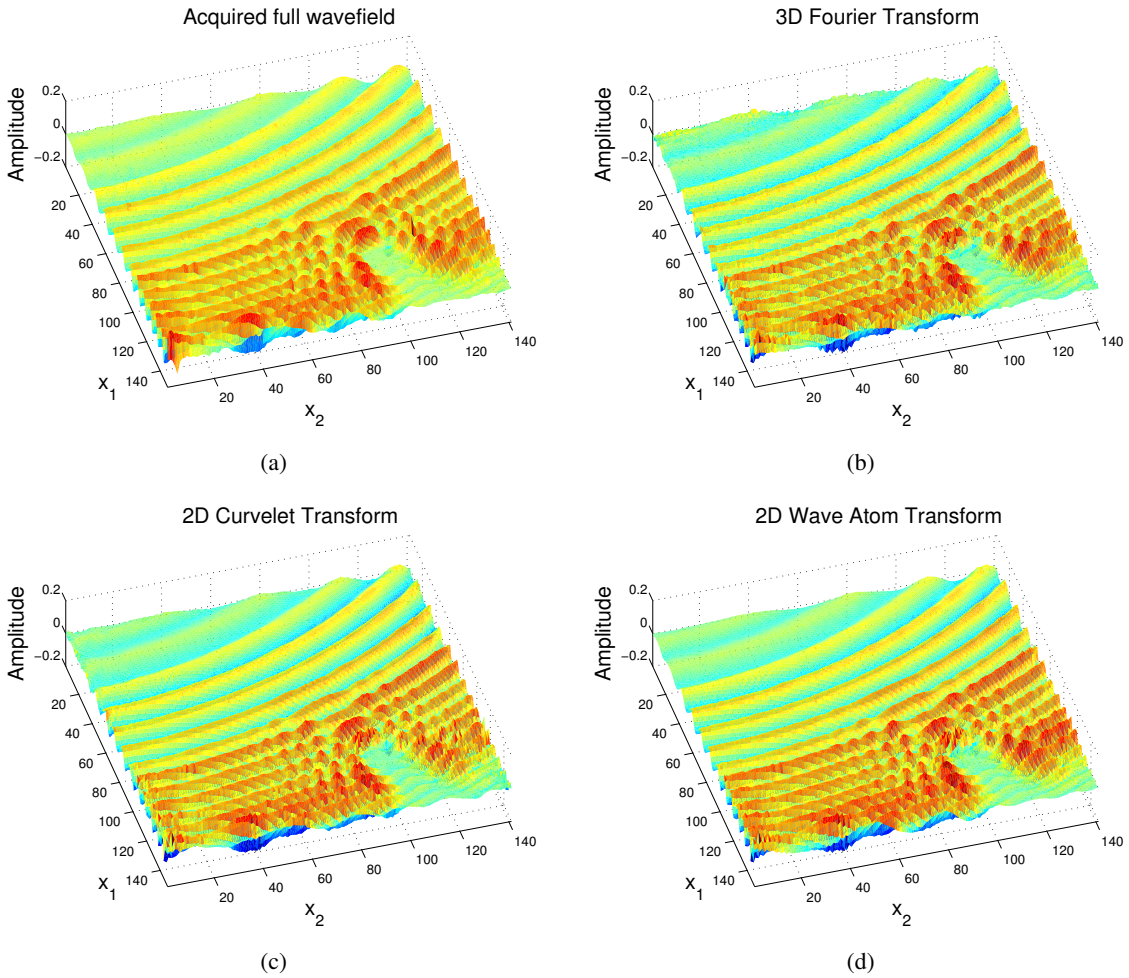

Figure 2: Wavefield image at a given instant of time t_j of the acquired full wavefield signal (a); and relative to the signal recovered in the 3D Fourier domain (b); 2D Curvelet domain (c); and Wave Atom domain (d) by less than 34% measurements respect to the original sampling grid.

suitable resolution and the computational cost in wavefield analysis purposes.

ACKNOWLEDGEMENTS

The research leading to these results has received funding from the SARISTU project (Grant Agreement no. 284562).

REFERENCES

[1] J. L. Rose. A baseline and vision of ultrasonic guided wave inspection potential. *Journal of Pressure Vessel Technology*, 124:273–282, August 2002.

[2] W. Staszewski, B. Lee, L. Mallet, and F. Scarpa. Structural health monitoring using scanning vibrometry: I. lamb wave sensing. *Smart Materials and Structures*, 13(2):251–260, February 2004.

[3] E. Candès and M. Wakin. An introduction to compressive sampling. *IEEE Signal Processing Magazine*, 25(2):21–30, March 2008.

[4] J. Ma and G. Plonka. The curvelet transform. *IEEE Signal Processing Magazine*, 27(2):118–133, March 2010.

[5] L. Demanet and L. Ying. Wave atoms and sparsity of oscillatory patterns. *Applied and Computational Harmonic Analysis*, 23(3):368–387, November 2007.

[6] T. E. Michaels, J. E. Michaels, and M. Ruzzene. Frequency-wavenumber domain analysis of guided wavefields. *Ultrasonics*, 51(4):452–466, November 2011.

[7] M. Ruzzene. Frequency-wavenumber domain filtering for improved damage visualization. *Smart Materials and Structures*, 16:2116–2129, October 2007.

[8] E. Candès, L. Demanet, D. Donoho, and L. Ying. Fast discrete curvelet transforms. Technical report, Applied and Computational Mathematics, California Institute of Technology, 2005.

[9] D. L. Donoho. Compressed sensing. *IEEE Transactions on Information Theory*, 52(4):1289–1306, April 2006.

[10] G. Hennefent and F. J. Herrmann. Simply denoise: wavefield reconstruction via jittered under-sampling. *Geophysics*, 73(3):19–28, May 2008.

[11] R. Shahidi, G. Tang, J. Ma, and F. J. Herrmann. Application of randomized sampling schemes to curvelet-based sparsity-promoting seismic data recovery. *Geophysical Prospecting*, 61(5):973–997, September 2013.

[12] E. van den Berg and M. P. Friedlander. Probing the pareto frontier for basis pursuit solutions. *SIAM J. on Scientific Computing*, 31(2):890–912, November 2008.

[13] E. van den Berg, M. P. Friedlander, F. J. Herrmann, R. Saab, and O. Yilmaz. Sparco: A testing framework for sparse reconstruction. Technical report, Department of Computer Science, University of British Columbia, 2007.